IEEE Access
Multidisciplinary ⋮ Rapid Review ⋮ Open Access Journal

Received 25 April 2024, accepted 26 May 2024, date of publication 5 June 2024, date of current version 13 June 2024.

Digital Object Identifier 10.1109/ACCESS.2024.3409741

RESEARCH ARTICLE

GRU-Based Fusion Models for Enhanced Blood Pressure Estimation From PPG Signals

SYAMSUL RIZAL[1,2], (Member, IEEE), AND YUNIARTI ANA RAHMA[3], (Member, IEEE)
[1]School of Electrical Engineering, Telkom University, Bandung 40257, Indonesia
[2]ICT Convergence Research Center, Kumoh National Institute of Technology, Gumi 39177, South Korea
[3]Department of Computer Engineering, Universitas Pendidikan Indonesia, Bandung 40154, Indonesia

Corresponding author: Syamsul Rizal (syamsul@telkomuniversity.ac.id)

This work was supported in part by the Faculty of Electrical Engineering for facilitating this research, and in part by the Directorate of Research and Community Service at Telkom University, Bandung.

ABSTRACT The current study presents a novel, non-invasive method for estimating both systolic and diastolic blood pressure by combining photoplethysmogram (PPG) signals with physiological data, such as sex, age, weight, height, heart rate, and BMI, using two Gated Recurrent Units (GRUs) models. The first model processes dynamic patterns in PPG signals, while the second model incorporates physiological parameters. Both models are connected through a series of dense layers. To prepare the datasets for the GRU framework, rigorous preprocessing was conducted. This resulted in a robust architecture capable of accurately predicting systolic and diastolic blood pressure. The proposed method achieved a Mean Absolute Error (MAE) of 1.458 for systolic and 1.164 for diastolic blood pressure. These findings demonstrate the potential of this approach for continual and non-intrusive blood pressure monitoring in wearable health technology. The study's results also make a significant contribution to the field of medical monitoring technology. The proposed solution addresses a major limitation in traditional blood pressure measurement practices and paves the way for advancements in personalized health monitoring, particularly for managing hypertension and cardiovascular conditions.

INDEX TERMS Blood pressure, deep learning, gated recurrent units (GRU), neural networks, photoplethysmography (PPG).

I. INTRODUCTION

Estimating blood pressure (BP) accurately is crucial for monitoring and managing cardiovascular health [1]. Traditional techniques for measuring blood pressure (BP) typically involve invasive methods that, while highly accurate, may pose certain risks such as infection, local bleeding, and vascular injury, particularly when continuous monitoring is required [2]. Non-invasive methods have been developed to address these limitations, with photoplethysmography (PPG) emerging as a promising alternative to estimate BP without causing harm. PPG signals, obtained through optical sensors that measure the light reflected from blood vessels, provide information about the volume changes in blood that occur during the cardiac cycle [3], [4], [5], [6].

Machine learning and deep learning methods have greatly improved the analysis of blood pressure using PPG signals. These methods utilize the structural features and frequency components of PPG signals to predict blood pressure with a high level of accuracy that is close to clinical standards. However, the practical application of electrocardiography (ECG) signals in blood pressure monitoring is hindered by artifacts caused by non-constrained environments, such as motion, electrode misplacement, and baseline wander. Although machine learning models and advanced signal processing techniques have been proposed to address these issues, challenges remain, including large mean absolute error (MAE) values and the time-consuming task of manually tuning hyperparameters in deep learning models, which can lead to potential performance inefficiencies and increased computational demands [7], [8].

The associate editor coordinating the review of this manuscript and approving it for publication was Manuel Rosa-Zurera.

In light of the previously mentioned difficulties, we suggest a novel strategy that employs dual Gated Recurrent Unit (GRU) models to process PPG signals together with demographic data, including age, gender, weight, height, heart rate, and body mass index (BMI), with the goal of improving blood pressure (BP) prediction. This method addresses the issues of hyperparameter tuning and computational efficiency by incorporating automated hyperparameter optimization techniques. Moreover, we propose that the integration of demographic information enhances the model's capacity to capture individual physiological variations that affect BP readings.

Our proposed models are assessed against the rigorous standards established by the Association for the Advancement of Medical Instrumentation (AAMI), the British Hypertension Society (BHS), and the Institute of Electrical and Electronics Engineers (IEEE), ensuring that our results align with recognized guidelines for medical devices and algorithms. This study aims to advance the field of BP monitoring by presenting a method that not only simplifies the process of BP estimation but also improves its reliability and applicability in daily healthcare management.

II. RELATED WORKS

The non-invasive blood pressure estimation landscape is constantly evolving, and recent research has heavily relied on PPG signals due to their potential for continuous monitoring applications. Hasanzadeh et al. proposed a machine learning model that emphasized the morphological features of PPG signals for BP estimation by focusing on characteristics such as systolic and diastolic peaks. This approach resulted in substantial improvements in accuracy, demonstrating the importance of extracting detailed signal features for precise blood pressure prediction [9].

Ibtehaz et al. proposed a novel approach using the PPG2ABP model, a cascaded deep learning framework designed for continuous arterial blood pressure waveform estimation from PPG signals. This method eliminated the need for handcrafted features, a common limitation in previous studies, and adhered to BHS and AAMI standards, demonstrating its potential for clinical applications [10].

Mahardika et al. investigated the potential of a convolutional long short-term memory (CNN-LSTM) neural network by employing grid search for hyperparameter optimization. Their research, which utilized the MIMIC III dataset, exhibited impressive accuracy in estimating systolic and diastolic BP, meeting the criteria set by BHS, AAMI, and IEEE. However, the study emphasized the need for larger datasets to validate long-term monitoring [11].

Slapnicar et al. developed a deep neural network with residual connections to analyze PPG signals and their derivatives, using data from the MIMIC III database. The study achieved notable accuracy in BP estimation but highlighted the need to personalize models for improved results, despite the high computational demand [12].

The research conducted by Zhang et al. highlights the significance of non-invasive ambulatory blood pressure (ABP) monitoring in averting cardiovascular diseases, while simultaneously acknowledging the shortcomings of current ABP devices, such as their cost, discomfort, and inaccuracy. As an alternative, the authors propose a machine learning-based approach that employs Support Vector Machine (SVM) for nonlinear regression analysis of ABP from PPG signals.

To build a reliable and effective prediction model, the researchers examined over 7000 samples from the University of Queensland Vital Signs Dataset. They successfully minimized the number of PPG feature parameters from 21 to 9, enhancing accuracy and streamlining algorithm complexity. Although the study achieved reasonable results in blood pressure estimation using SVM, further improvements in accuracy are required to satisfy medical standards. Future work will concentrate on acquiring more standardized PPG signals, optimizing the SVM-training model with larger datasets, and implementing outlier removal techniques to improve prediction accuracy [13].

The potential use of GRU models in health-related situations, particularly in predicting blood pressure (BP) from PPG signals and patient demographic information, is a promising area for further investigation. Although GRU models have shown their ability to work with time-series data, their potential for interpreting PPG signals and patient-specific information for BP prediction has not yet been fully realized [14], [15]. This gap in research presents an opportunity for our dual-GRU model approach, which aims to integrate PPG signal analysis with patient-specific data to address the limitations identified in previous studies and advance the field of non-invasive BP monitoring.

III. METHODOLOGY

A. DATA COLLECTION

The dataset provided by Liang et al. in their study is a valuable resource for non-invasive CVD detection, encompassing 657 data segments from 219 individuals. This dataset, which encompasses a wide age range and includes conditions such as hypertension and diabetes, was carefully collected at the Guilin People's Hospital in China under controlled experimental conditions. The aim of this dataset is to investigate the quality of PPG signals and to explore their inherent connection to cardiovascular health, providing new opportunities for early and non-invasive screening of common CVDs like hypertension and diabetes, as reported in [16].

The custom-designed portable hardware platform, which integrated a PPG sensor probe, microcontroller, and compatible application, was utilized to acquire data. This platform enabled the simultaneous collection of PPG waveform signals and arterial blood pressure, ensuring high precision and quality of the PPG signals, which are crucial for accurate blood pressure estimation using only PPG signals. The PPG sensor utilized two LED lights at specific wavelengths and

transmitted the data through Bluetooth. The PPG detection probe used infrared light and transmission method to obtain fingertip PPG waveform data, which were then assessed for quality before being saved.

In addition to the dataset by Liang et al., PPG signals and corresponding patient information were collected from 25 patients in the MIMIC III matched subset and clinical database for comparative analysis. The use of the MIMIC III data, which involves a matched subset of patients, allows for a comprehensive comparison between datasets, offering insights into the variability of PPG signal quality and its implications for Blood Pressure estimation across different populations and clinical settings.

The controlled environment in which the comprehensive data collection process was conducted was critical to obtain authentic, high-precision, and high-quality PPG signals. This stringent approach to data collection and signal quality evaluation was necessary to ensure that the dataset contained complete heartbeat cycles with minimal noise and artifacts. However, the study acknowledges the challenges in acquiring rich PPG signals and extracting subtle characteristics that may indicate various physiological states or conditions.

B. PREPROCESSING

The preprocessing phase is a critical component of our research, as it entails refining both PPG signals and personal data ahead of the application of Gated Recurrent Unit (GRU) models. Prior to analysis, raw PPG waveforms derived from the PPGBP Database undergo a custom-designed bandpass filter, which employs a combination of high-pass and low-pass Butterworth filters. These filters are specifically calibrated to the frequency characteristics of the PPG signals to ensure optimal filtering.

The high-pass filter has a lower cutoff frequency set at 0.5 Hz, which is designed to eliminate low-frequency noise, such as baseline wander, that can obscure the true PPG signal. Conversely, the upper cutoff frequency for the low-pass filter is set at 15.0 Hz, which is chosen to eliminate high-frequency noise, such as electronic interference and motion artifacts, while preserving the essential components of the PPG signal related to blood pressure fluctuations. These filter settings are carefully selected based on the sampling frequency of the PPG data, which is 1000 Hz, to ensure that the filtering process is optimized for the accurate detection of blood flow-related features.

The output of the bandpass filtering process is a series of PPG signals with an enhanced signal-to-noise ratio, which are necessary for the subsequent feature extraction and pattern recognition stages. Moreover, the personal data, such as sex, age, height, weight, heart rate, and BMI, are normalized to establish a consistent scale for analysis. The normalization process is determined using equation (1). The preprocessed data is then divided into separate datasets for training, validation, and testing, as illustrated in Figure 1. This step ensures that the GRU models are trained on diverse data (60%), validated (25%), and tested (15%) on unseen data,

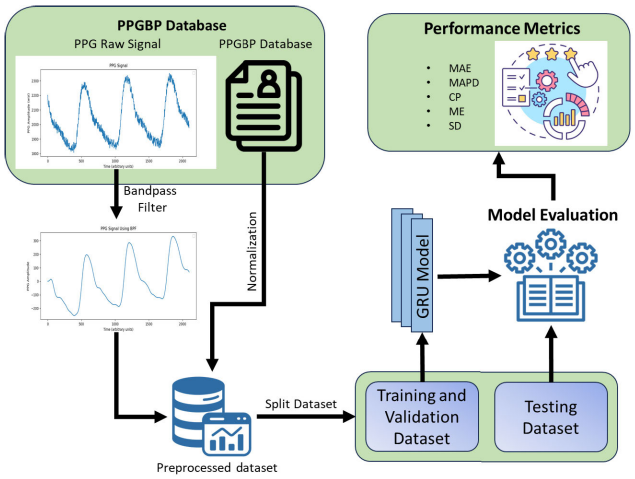

FIGURE 1. Schematic representation of the data preprocessing and GRU model evaluation pipeline.

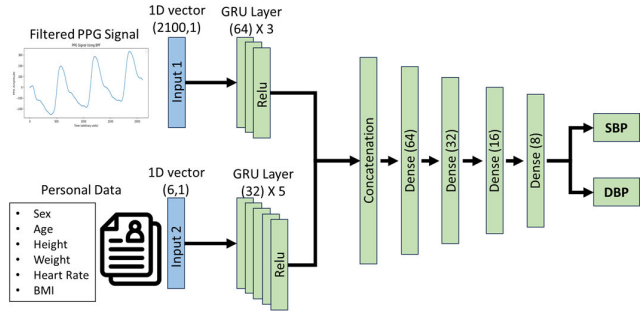

FIGURE 2. GRU-based model architecture for blood pressure estimation.

which is important for assessing the models' performance and generalizability.

$$X_{Normalized} = \frac{X - X_{min}}{X_{max} - X_{min}}. \tag{1}$$

C. MODEL ARCHITECTURE

The proposed model's architecture is depicted in Figure 2. Our study introduces a novel dual-input model design that incorporates Gated Recurrent Units (GRUs) to forecast systolic and diastolic blood pressure using preprocessed PPG signals and personal demographic data. This architecture is carefully crafted to seamlessly handle the time-series nature of PPG signals and the static nature of personal data, thereby effectively merging these diverse data types to deliver a comprehensive estimation of blood pressure.

The architecture of the current model is designed to handle temporally complex PPG data, which requires sequential data processing to capture the underlying patterns associated with Blood Pressure (BP). To achieve this, the model is composed of a series of Gated Recurrent Unit (GRU) layers. The PPG pathway specifically starts with a one-dimensional (1D) input vector of size (2100, 1), which contains the signal's time-steps and features. This input vector is then fed into three successive GRU layers, each consisting of 64 units, which employ Rectified Linear Unit (ReLU) activation functions to introduce non-linearity and facilitate the learning of intricate

patterns within the data. The choice of GRU layers is motivated by their ability to mitigate the vanishing gradient problem, which is common in recurrent networks, thereby enhancing the model's ability to learn from long sequences.

Moreover, in addition to processing the PPG signals, the model also processes personal demographic data, including sex, age, height, weight, heart rate, and Body Mass Index (BMI), through a separate input vector of size (6,1). This input vector is directed through a distinct series of five GRU layers, each comprising of 32 units, to capture the nuanced effects of these demographic variables on blood pressure.

Using separate processing paths, the output of both the gated recurrent unit (GRU) streams is combined through a concatenation layer, integrating the extracted features from PPG signals with demographic data. This concatenated output then undergoes a series of dense, fully connected layers, gradually decreasing in the number of units (64, 32, 16, and ultimately 8). These layers play a crucial role in recognizing patterns and making decisions, transforming the learned representations into accurate predictions for systolic blood pressure (SBP) and diastolic blood pressure (DBP).

The final layer of the architecture consists of two units, each corresponding to one of the target variables: SBP and DBP. This layer represents the culmination of the model's design and provides blood pressure estimates based on the complex relationship between PPG-derived features and personal demographic information. This advanced architecture demonstrates the potential of hybrid neural networks in tackling intricate biomedical prediction tasks, such as non-invasive blood pressure estimation.

D. HYPERPARAMETER FOR TRAINING

The training procedure for our proposed dual-input GRU-based model was rigorously developed to ensure effective learning from both PPG signals and demographic data. This process involved a deliberate selection of hyperparameters to balance the model's ability to discern complex patterns and avoid overfitting, as detailed in Table 1.

Employing the Adamax optimizer, renowned for its resilience in situations involving sparse gradients, our model profits from adaptive adjustments to the learning rate that address the ever-changing requirements of the data, thereby promoting stable convergence. By setting the learning rate at 0.005, we achieved an optimal balance between expeditious training and accurate weight modifications.

Our primary loss function, Mean Squared Error (MSE), demonstrates exceptional proficiency in evaluating the degree of discrepancy between forecasted and actual blood pressure measurements, placing a premium on precision, which is of paramount importance in medical contexts where the tolerance for error is narrow.

Our analysis revealed that a batch size of 128 strikes an optimal balance between computational efficiency and sample size sufficiency for precise gradient estimation through vectorized operations, thereby ensuring a more seamless training process.

TABLE 1. Hyperparameter proposed model.

Parameter	Value
Optimizer	Adamax
Learning Rate	0.005
Loss Function	MSE
Batch Size	128
Activation Function (Output Layer)	Linear
Epochs	500
Callback Function	Save Best Weight

The output layer of our model employs a linear activation function, which is ideally suited for regression tasks that involve predicting continuous variables like systolic blood pressure (SBP) and diastolic blood pressure (DBP). This function enables the model to generate a wide range of blood pressure values.

The incorporation of a comprehensive training regimen consisting of 500 epochs was crucial in providing the model with ample opportunity to learn from the data thoroughly. Additionally, a callback function was employed to monitor the validation loss and preserve only the best weights, which correspond to the highest accuracy on the validation set. This strategy is effective in mitigating overfitting by halting training when the model's performance on the validation set ceases to improve, thereby signifying convergence.

After concluding the training phase, the model was subjected to extensive testing on a previously unseen dataset to evaluate its ability to generalize and its suitability for implementation in real-world clinical settings. This final evaluation is critical in confirming the model's predictive capabilities and its preparedness for use in non-invasive blood pressure monitoring.

IV. EXPERIMENTS AND RESULTS

A. EXPERIMENTAL SETUP

Our experimental setup was carefully designed to ensure the dependability and reproducibility of our results. We employed a structured approach to dividing our dataset, which consists of three subsets: Training, Validation, and Testing. Each subset serves a specific purpose in the development and assessment of our model. The Training set, comprising 60% of the total data, is used to fit the model and adjust the neural network's weights. The Validation set, representing 25% of the data, is used to fine-tune the model parameters and prevent overfitting, acting as a pseudo-test set to provide an early indication of the model's performance during the training phase. Finally, the Testing set, also 15% of the data, is used to evaluate the model's predictive power. This separation ensures that the model is assessed on entirely unseen data, providing an impartial measure of its generalization capabilities.

To evaluate the performance of our proposed model, we have selected a comprehensive set of metrics based on three well-established standards: IEEE, BHS, and AAMI standards, providing a thorough analysis of its predictive accuracy and dependability.

1) IEEE STANDARD

The Institute of Electrical and Electronics Engineers (IEEE) standard is focused on the accuracy and dependability of cuffless, wearable blood pressure monitoring devices. In this study, we utilize the following metrics in accordance with the IEEE standard. The Mean Absolute Error (MAD) is determined using equation (2), which calculates the average magnitude of errors between predicted and actual values, without regard to their direction. Furthermore, the Mean Absolute Percentage Difference (MAPD) is calculated using equation (3), which provides a normalized measure of error relative to the magnitude of the true values, enabling comparisons across various scales [17].

$$MAD = \frac{1}{n}\sum_{i=1}^{n}\left|y_i - \hat{y}_i\right|. \tag{2}$$

$$MAPD = \frac{100\%}{n}\sum_{i=1}^{n}\left|\frac{y_i - \hat{y}_i}{y_i}\right|. \tag{3}$$

2) BHS STANDARD

The British Hypertension Society (BHS) uses a standardized grading system to assess the accuracy of blood pressure measurement devices by determining the proportion of readings that fall within predetermined error thresholds. The BHS employs the equation (4), which calculates the cumulative percentages (CP), to reflect the percentage of predictions that fall within specific margins of error relative to the true blood pressure values. This established standard allows for a precise evaluation of the precision of blood pressure measurement devices [18].

$$CP = \frac{CummulativeFrequency}{n} \times 100. \tag{4}$$

3) AAMI STANDARD

The Association for the Advancement of Medical Instrumentation (AAMI) standard provides guidelines for the mean and variability of blood pressure measurement errors. In order to comply with this standard, we focus on calculating the Mean Error (ME) and Standard Deviation (SD) using formulas (5) and (6) respectively [19].

$$ME = \frac{1}{n}\sum_{i=1}^{n}\left(y_i - \hat{y}_i\right). \tag{5}$$

$$SD = \sqrt{\frac{1}{n}\sum_{i=1}^{n}\left(y_i - \hat{y}_i - ME\right)^2}. \tag{6}$$

4) OTHER PERFORMANCE METRICS

As part of our comprehensive evaluation, we also computed the Mean Relative Error (MRE) and Root Mean Squared Error (RMSE) [20], [21], [22], [23].

The Mean Relative Error (MRE), expressed as a percentage, is a measure of the average relative error between predicted and actual values, as indicated by equation (7).

TABLE 2. Performance requirements for blood pressure estimation models according to IEEE, BHS, and AAMI standards.

Standard	Grade	Metrics		
		MAD (mmHg)		
IEEE	A	≤5		
	B	5-6		
	C	6-7		
	D	> 7		
BHS		CP 5 mmHg	CP 10 mmHg	CP 15 mmHg
	A	60%	85%	95%
	B	50%	75%	90%
	C	40%	65%	85%
	D	Lower than C		
AAMI		ME (mmHg)	SD (mmHg)	
	Pass	≤5	≤8	

This metric offers valuable information regarding the model's relative accuracy across varying scales of measurement.

$$MRE = \frac{1}{n}\sum_{i=1}^{n}\left|\frac{y_i - \hat{y}i}{yi}\right| \times 100 \tag{7}$$

The Root Mean Squared Error (RMSE), as calculated using equation (8), is a commonly employed metric that reflects the square root of the average squared differences between the predicted and actual values. It offers a comprehensive measure of the magnitude of the model's prediction error.

$$RMSE = \sqrt{\frac{1}{n}\sum_{i=1}^{n}(y_i - \hat{y}_i)^2}. \tag{8}$$

The inclusion of these additional metrics provides a comprehensive assessment of the model's performance, incorporating both absolute and relative error measures.

Table 2, outlines the grading criteria for blood pressure estimation models as defined by the IEEE, BHS, and AAMI standards. According to the IEEE standard, model accuracy is classified into grades A to D, with Grade A requiring a Mean Absolute Error (MAE) of less than 5 mmHg and Grade D indicating a MAE higher than 7 mmHg. The BHS standard grades models based on the Cumulative Percentages (CP) of predictions within 5, 10, and 15 mmHg of the true blood pressure values, with a minimum of 60% of predictions within 5 mmHg required for Grade A. Lastly, the AAMI standard sets a pass threshold for the Mean Error (ME) of less than 5 mmHg and the Standard Deviation (SD) of errors to be less than 8 mmHg, ensuring that the model's predictions are both accurate and consistent.

B. RESULTS

Table 3 provides a thorough assessment of the performance of various machine learning models in estimating Systolic Blood Pressure (SBP) and Diastolic Blood Pressure (DBP) using Photoplethysmography (PPG) signals. The table showcases an extensive range of neural network architectures and machine learning methods, such as Convolutional Neural

Networks (CNN)-Long Short-Term Memory (LSTM), Support Vector Machines (SVM), Residual Neural Networks (ResNet), Artificial Neural Networks (ANN), Recurrent Neural Networks (RNN), and U-Net, as well as ensemble methods like AdaBoost. The evaluation of performance is based on Mean Absolute Error (MAE) and Standard Deviation (SD) metrics, which are indicative of the models' accuracy and consistency, respectively. Each entry in the table offers specific information about the study, including the machine learning method, the input data type (PPG), the dataset used for evaluation (including MIMIC III, MIMIC II, Queensland, UCI), and the MAE and SD for both SBP and DBP.

The concluding entry in the table showcases the proposed model, which incorporates a dual GRU network and an ANN, and employs both PPG and demographic data. This model was initially evaluated on the PPGBP dataset, achieving notably low mean absolute error (MAE) values for systolic blood pressure (SBP) and diastolic blood pressure (DBP) of 1.45 and 1.16, respectively. The corresponding standard deviation (SD) values for SBP and DBP were 2.658 and 1.628, respectively, indicating improved accuracy and consistent performance.

The GRU and Dense model displayed mean absolute error (MAE) values of 5.74 for systolic blood pressure (SBP) and 6.72 for diastolic blood pressure (DBP) when applied to the MIMIC III dataset. The standard deviation (SD) values for SBP and DBP were 6.97 and 8.93, respectively. These results indicate a decline in performance compared to the PPGBP dataset, but they provide useful information about the model's ability to generalize and potential areas for improvement. The higher MAE and SD values suggest that further model adjustments may be necessary to account for the unique characteristics of the MIMIC III dataset, which may include a more diverse patient population or distinct PPG signal patterns.

Furthermore, the versatility and robustness of the proposed model have been substantiated through additional results from the MIMIC III dataset, which demonstrate an average absolute error (MAE) of 1.42 for systolic blood pressure (SBP) and 1.97 for diastolic blood pressure (DBP), along with standard deviation (SD) values of 2.38 for SBP and 2.97 for DBP. These findings highlight the model's generalizability and its potential to provide accurate blood pressure estimates across various datasets. The slight increase in SD when applied to the MIMIC III dataset indicates a variation in the estimates that may necessitate further investigation to improve the model's predictive consistency.

Figure 3 illustrates a set of scatter plots contrasting the true versus estimated blood pressure (BP) levels for both systolic (SBP) and diastolic (DBP) readings. Each plot comprises individual data points portraying the actual BP recorded versus the BP predicted by a model.

In the first plot dedicated to SBP (left side), the blue dots represent individual predictions, with the x-axis representing the actual SBP and the y-axis showing the predicted SBP.

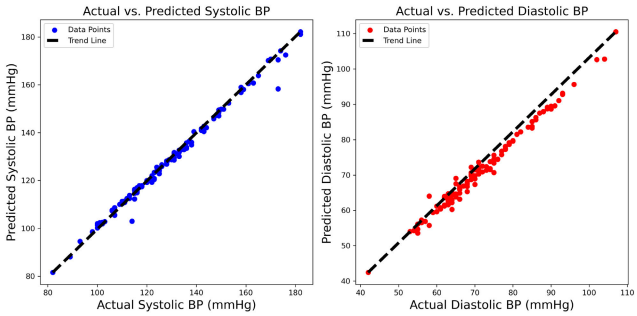

FIGURE 3. Scatter plots of actual vs. Predicted blood pressure values: SBP (left) and DBP (right).

The dashed trend line indicates a strong positive correlation between the actual and predicted values, signifying that the model demonstrates exceptional accuracy in predicting SBP across a broad spectrum of measurements.

The second plot on the right shows individual predictions for DBP, represented by red dots on the graph. The x-axis represents the actual DBP values, while the y-axis represents the predicted DBP values. The trend line in the plot displays a strong positive correlation, indicating that the model's predictions for DBP are accurate as well.

The alignment of the data points along the trend lines in both plots, which are nearly 45 degrees, suggests that the model's predictions are close to the actual values. This implies that the model performs well for both SBP and DBP predictions.

However, it is important to note that without numerical data or statistical analysis (e.g., correlation coefficients, R-squared values), we cannot quantify the exact accuracy or potential discrepancies between the predicted and actual BP readings. Although the plots do not show any extreme outliers or systematic bias, a comprehensive evaluation of the model's performance requires analyzing the plots in conjunction with the actual numerical results.

The figure presented in Figure 4 offers a comprehensive examination of a blood pressure estimation model's performance through two Bland-Altman plots and two histograms. Regarding the SBP, the Bland-Altman plot displays a mean difference of 0.84 mmHg between the actual and predicted values, which indicates a negligible average bias in the model's forecasts. The upper limit of agreement is 6.05 mmHg, and the lower limit is −4.37 mmHg, as depicted in Figure 4a. These boundaries represent the range within which 95% of the differences between the actual and predicted SBP values can be found. The relatively small mean difference and narrow limits of agreement suggest that the model demonstrates a high level of precision in predicting SBP, with most discrepancies falling within a clinically acceptable range.

The Bland-Altman plots show that the model's predictions for DBP are highly accurate, with a mean difference of only 0.04 mmHg, indicating a negligible bias. This suggests that the model's predictions are, on average, very close to the actual DBP measurements. The upper and lower limits

TABLE 3. Comparison of performance metrics evaluation with the existing works in estimating SBP and DBP.

References	Method	Input	Dataset	SBP		DBP	
				MAE	SD	MAE	SD
[11]	CNN_LSTM	PPG	MIMIC III	3.64	7.04	2.39	3.79
[24]	SVR	PPG	MIMIC II	8.54	-	4.34	-
[13]	SVM	PPG	Queensland	11.6	8.2	7.6	6.7
[12]	Spectro-temporal ResNet	PPG	MIMIC III	9.43	-	6.88	-
[25]	ANN	PPG	MIMIC II	9.74	12.40	4.65	6.29
[26]	RNN	PPG	MIMIC III	12.08	15.67	5.56	7.32
[10]	U-Net	PPG	MIMIC III	5.73	-	3.45	-
[27]	CNN	PPG	Private Dataset	-	14.03	-	-
[9]	AdaBoost	PPG	MIMIC II	8.22	10.38	4.17	4.22
[28]	CNN-BiLSTM	PPG	UCI (MIMIC II)	7.85	8.41	4.42	4.8
[29]	LightGBM	PPG	PPGBP	13.06	-	8.16	-
Proposed Model	GRU + Dense	PPG + Demographic	MIMIC III	5.74	6.97	6.72	8.93
Proposed Model	**Dual GRU + ANN**	**PPG + Demographic**	**PPGBP MIMIC III**	**1.45** **1.42**	**2.658** **1.97**	**1.16** **2.38**	**1.628** **2.97**

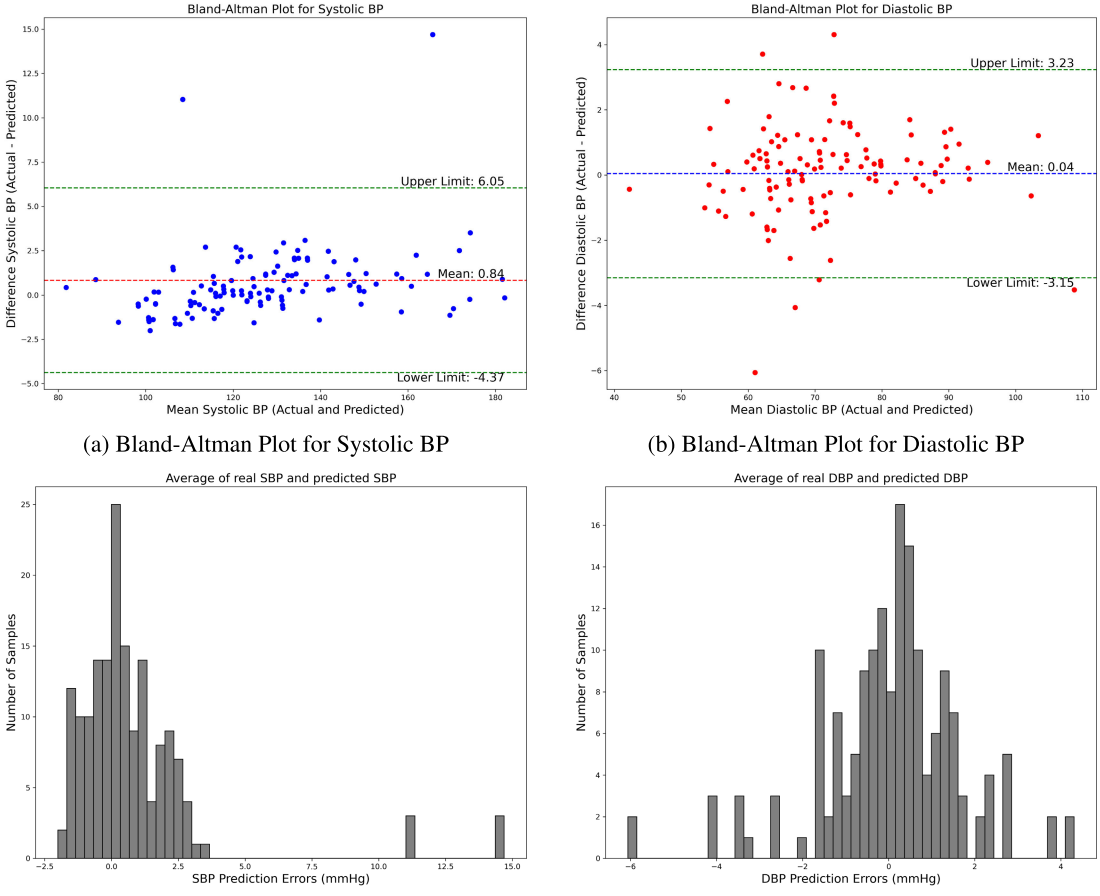

(a) Bland-Altman Plot for Systolic BP

(b) Bland-Altman Plot for Diastolic BP

(c) Histogram of SBP Prediction Errors

(d) Histogram of DBP Prediction Errors

FIGURE 4. Comprehensive analysis of blood pressure estimation accuracy.

of agreement for DBP are 3.23 mmHg and −3.15 mmHg, respectively, as shown in Figure 4b. These limits are tighter than those for SBP, indicating higher precision in the model's DBP predictions. Overall, the Bland-Altman plots demonstrate the model's high accuracy and reliability in estimating both SBP and DBP, making it a promising candidate for non-invasive blood pressure monitoring in clinical settings.

The Bland-Altman plots are supplemented by histograms, which visually depict the distribution of prediction errors. The shape, central tendency, and spread of the histograms provide valuable information about the error characteristics of the model. A symmetrical histogram centered on the zero-axis suggests that the model is unbiased, equally likely to overestimate or underestimate the blood pressure. Conversely, if the histogram is skewed or deviates from the center,

TABLE 4. Performance metrics for systolic and diastolic blood pressure prediction.

Metric	Systolic BP	Diastolic BP
MAE (mmHg)	1.459	1.165
MRE (%)	1.114	1.687
RMSE (mmHg)	2.787	1.628
MAPD (%)	1.114	1.687
CP within 5 mmHg (%)	96.364	98.788
CP within 10 mmHg (%)	96.364	100.000
CP within 15 mmHg (%)	100.000	100.000
ME (mmHg)	0.840	0.041
SD (mmHg)	2.658	1.628

it indicates systematic overprediction or underprediction. The width of the histogram indicates the range of errors and reflects the accuracy and dependability of the model.

These plots allow for a comprehensive evaluation of the model. They show not only the average difference between the predictions and the true values (bias), but also the range and precision of the predictions. They are particularly useful for determining the reliability of the model at different blood pressure levels and identifying any systematic errors that need to be addressed to improve the model's accuracy and clinical applicability.

Table 4 presents key performance metrics of the proposed model for predicting Systolic Blood Pressure (SBP) and Diastolic Blood Pressure (DBP). The model achieves a Mean Absolute Error (MAE) of 1.459 mmHg for SBP and 1.165 mmHg for DBP, indicating a low average absolute difference between predicted and actual values. The Mean Relative Error (MRE) is 1.114% for SBP and 1.687% for DBP, reflecting a small relative difference between predictions and actual measurements. Additionally, the Root Mean Squared Error (RMSE) is 2.787 mmHg for SBP and 1.628 mmHg for DBP, demonstrating the model's precision, with slightly higher variability in SBP predictions. These metrics highlight the model's accuracy and reliability in predicting blood pressure values, showing low error rates and high consistency in its performance.

Table 5 provides a comprehensive assessment of the proposed technique for predicting SBP and DBP, evaluated against three widely-acknowledged benchmarks: IEEE, BHS, and AAMI, using a range of precision metrics. The IEEE Standard's Mean Absolute Error (MAE) and Mean Absolute Percentage Difference (MAPD) measurements demonstrate the model's accuracy. With an SBP MAE of 1.459 mmHg and DBP MAE of 1.165 mmHg, the model easily surpasses the demanding criteria of the standard. As a result, the model is awarded an 'A' grade for both SBP and DBP, along with MAPD values of 1.114% for SBP and 1.687% for DBP.

In accordance with the BHS Standard, which assesses the precision of blood pressure projections through Cumulative Percentages (CP) at intervals of 5, 10, and 15 mmHg, the model's predictions for SBP and DBP exceed 96% and 98% accuracy, respectively, within a 5 mmHg margin. This performance results in a perfect score of 100% for both SBP and DBP predictions within the 15 mmHg range, and thus, the model earns another set of 'A' grades for its accuracy in predicting both SBP and DBP.

Evaluations conducted in accordance with the AAMI Standard, which assesses the Mean Error (ME) and the Standard Deviation of the error (SD), indicate a minimal bias with ME values of 0.84 mmHg for SBP and a noteworthy 0.041 mmHg for DBP. The SD values reflect the consistency, with 2.658 mmHg for SBP and 1.628 mmHg for DBP. These results align with the AAMI Standard's criteria, suggesting the model's dependability for clinical application.

Upon analyzing the PPGBP dataset, the model demonstrates impressive accuracy and reliability, as evidenced by its adherence to established standards. Furthermore, extending the model's assessment to the MIMIC III dataset reinforces its effectiveness; it displays a comparable mean absolute error of 1.429 mmHg for SBP and 2.385 mmHg for DBP. Although there is a slight increase in the MAPD and SD values–1.523% and 2.38 mmHg for SBP, and 4.208% and 2.97 mmHg for DBP, respectively—the model still maintains a consistently high level of performance, achieving an 'A' grade across the board. These additional metrics from the MIMIC III dataset underscore the model's versatility and its potential as a precise and accurate tool for non-invasive blood pressure monitoring.

V. DISCUSSION

Our investigation's outcomes indicate that the proposed dual-input GRU-based model demonstrates high accuracy and reliability in estimating blood pressure, as shown by the performance metrics assessed against IEEE, BHS, and AAMI standards. The Mean Absolute Error (MAE) and Mean Absolute Percentage Difference (MAPD) for both systolic and diastolic blood pressure estimation were well within the stringent requirements of the IEEE standard, earning a grade of 'A.' This suggests the model's high precision and minimal bias, which aligns with the IEEE's emphasis on accuracy for wearable, cuffless blood pressure monitoring devices.

Furthermore, the model's predictions were validated against the BHS standard, showing that over 96% of systolic and 98% of diastolic readings fell within a 5 mmHg range, with 100% within a 15 mmHg range. This exceptional performance earned the model a grade of 'A' under BHS criteria and emphasizes its potential for clinical application, considering that BHS grading is a recognized benchmark in evaluating the clinical utility of blood pressure monitoring devices.

The model in question has effectively fulfilled the AAMI standards, showing minimal bias as demonstrated by its ME values and consistent predictions as shown by its SE values across measurements. These results suggest that the model has the potential to be a dependable clinical tool for monitoring blood pressure, especially in situations where non-invasive, continuous measurement is preferred.

The model's exceptional accuracy and reliability can be attributed to its ability to account for temporal dependencies within PPG signals and its integration of personal

TABLE 5. Performance evaluation of the proposed method for SBP and DBP prediction based on the IEEE, BHS, and AAMI standards.

Assessment Evaluation	IEEE Standard			BHS Standard				AAMI Standard		
	MAD (≤4 mmHg)	MAPD (%)	Grade	CP5 (>60%)	CP10 (>85%)	CP15 (>95%)	Grade	ME (<5 mmHg)	SD (<8 mmHg)	Grade
PPGBP										
SBP	1.459	1.114	A	96.364	96.364	100	A	0.84	2.658	Pass
DBP	1.165	1.687	A	98.78	100	100	A	0.041	1.628	Pass
MIMIC III										
SBP	1.429	1.323	A	100	100	100	A	0.003	1.976	Pass
DBP	2.385	4.208	A	90.541	100	100	A	0.492	2.976	Pass

demographic data, which provides a more comprehensive understanding of the individual's cardiovascular health. The use of a dual-input system enables the model to learn from both PPG waveforms that change over time and personal health data that remains static, resulting in a more sophisticated approach to blood pressure estimation that surpasses many single-input models.

The outcomes of this study contribute to the expanding body of research on non-invasive methods for monitoring blood pressure and support the practicality of utilizing machine learning models, particularly those that incorporate GRU networks, for this application. However, it is essential to recognize potential limitations, such as the need for further validation on larger and more diverse datasets, and to evaluate the model's performance in real-world situations beyond controlled clinical environments.

Future research will concentrate on addressing these limitations by refining the model through additional feature engineering and exploring the integration of other physiological signals to enhance prediction accuracy. The ultimate goal is to develop a sturdy, non-invasive blood pressure monitoring system that can be implemented in various healthcare settings, from critical care to home-based monitoring, potentially improving patient outcomes and healthcare delivery.

VI. CONCLUSION

The research presented in this paper highlights the promising potential of machine learning, particularly Gated Recurrent Unit (GRU) networks, in improving non-invasive blood pressure monitoring technologies. Our dual-input GRU model, which integrates PPG signals and personal demographic data, has demonstrated a high level of accuracy and reliability. The model's performance, as evaluated against the IEEE, BHS, and AAMI standards, showcases its ability to accurately estimate systolic and diastolic blood pressure, as indicated by the low Mean Absolute Error (MAE), high Cumulative Percentages (CP) within clinically acceptable ranges, and compliance with the Mean Error (ME) and Standard Deviation (SE) criteria set by the AAMI standard.

The results of the study, demonstrated by the model's exceptional performance at the BHS standard and its fulfillment of the AAMI criteria, offer great potential for the field of wearable health technology and telemedicine. The successful integration of time-series PPG data with static personal health metrics into a cohesive model showcases the innovative use of GRU networks in medical diagnostics.

Moving forward, our findings establish a strong base for the ongoing development and refinement of non-invasive, continuous blood pressure monitoring systems. The practical applications of such advancements hold significant promise for enhancing patient care, allowing for more proactive and personalized healthcare management, especially for individuals with hypertension or those at risk of cardiovascular diseases.

This study offers valuable insights into the potential of advanced neural network architectures for monitoring vital signs. Additionally, it paves the way for future research that could result in the widespread application of these methods in clinical settings. Nevertheless, it is essential to conduct thorough and extensive testing of the model on various datasets to confirm its dependability and to assess the potential advantages of incorporating additional physiological factors that could enhance its predictive capabilities.

DATA AVAILABILITY STATEMENT

The datasets analyzed during the current study are available from the corresponding author on reasonable request. The source code for the model training, evaluation, and additional materials supporting the findings of this study have been made available on Code Ocean, a platform that ensures computational reproducibility. The source code can be accessed at the following link: https://codeocean.com/capsule/8144631/tree/v1.

REFERENCES

[1] T. Hansen, J. Jeppesen, S. Rasmussen, H. Ibsen, and C. Torppedersen, "Ambulatory blood pressure monitoring and risk of cardiovascular disease: A population based study," *Amer. J. Hypertension*, vol. 19, no. 3, pp. 243–250, Mar. 2006.

[2] Z. Liu, C. Zhou, H. Wang, and Y. He, "Blood pressure monitoring techniques in the natural state of multi-scenes: A review," *Frontiers Med.*, vol. 9, Aug. 2022, Art. no. 851172.

[3] X. Xing, Z. Ma, M. Zhang, Y. Zhou, W. Dong, and M. Song, "An unobtrusive and calibration-free blood pressure estimation method using photoplethysmography and biometrics," *Sci. Rep.*, vol. 9, no. 1, Jun. 2019, Art. no. 8611.

[4] M. Ghamari, "A review on wearable photoplethysmography sensors and their potential future applications in health care," *Int. J. Biosensors Bioelectron.*, vol. 4, no. 4, 2018, Art. no. 195.

[5] K. Azudin, K. B. Gan, R. Jaafar, and M. H. Ja'afar, "The principles of hearable photoplethysmography analysis and applications in physiological monitoring—A review," *Sensors*, vol. 23, no. 14, p. 6484, Jul. 2023.

[6] H. W. Loh, S. Xu, O. Faust, C. P. Ooi, P. D. Barua, S. Chakraborty, R.-S. Tan, F. Molinari, and U. R. Acharya, "Application of photoplethysmography signals for healthcare systems: An in-depth review," *Comput. Methods Programs Biomed.*, vol. 216, Apr. 2022, Art. no. 106677.
[7] M. M. R. K. Mamun and A. Sherif, "Advancement in the cuffless and noninvasive measurement of blood pressure: A review of the literature and open challenges," *Bioengineering*, vol. 10, no. 1, p. 27, Dec. 2022.
[8] S. N. A. Ismail, N. A. Nayan, R. Jaafar, and Z. May, "Recent advances in non-invasive blood pressure monitoring and prediction using a machine learning approach," *Sensors*, vol. 22, no. 16, p. 6195, Aug. 2022.
[9] N. Hasanzadeh, M. M. Ahmadi, and H. Mohammadzade, "Blood pressure estimation using photoplethysmogram signal and its morphological features," *IEEE Sensors J.*, vol. 20, no. 8, pp. 4300–4310, Apr. 2020.
[10] N. Ibtehaz, S. Mahmud, M. E. H. Chowdhury, A. Khandakar, M. S. Khan, M. A. Ayari, A. M. Tahir, and M. S. Rahman, "PPG2ABP: Translating photoplethysmogram (PPG) signals to arterial blood pressure (ABP) waveforms," *Bioengineering*, vol. 9, no. 11, p. 692, Nov. 2022.
[11] N. Q. Mahardika T, Y. N. Fuadah, D. U. Jeong, and K. M. Lim, "PPG signals-based blood-pressure estimation using grid search in hyperparameter optimization of CNN–LSTM," *Diagnostics*, vol. 13, no. 15, p. 2566, Aug. 2023.
[12] G. Slapničar, N. Mlakar, and M. Luštrek, "Blood pressure estimation from photoplethysmogram using a spectro-temporal deep neural network," *Sensors*, vol. 19, no. 15, p. 3420, Aug. 2019.
[13] Y. Zhang and Z. Feng, "A SVM method for continuous blood pressure estimation from a PPG signal," in *Proc. 9th Int. Conf. Mach. Learn. Comput.*, Feb. 2017, pp. 128–132.
[14] M. A. Morid, O. R. L. Sheng, and J. Dunbar, "Time series prediction using deep learning methods in healthcare," *ACM Trans. Manage. Inf. Syst.*, vol. 14, no. 1, pp. 1–29, Jan. 2023.
[15] P. B. Weerakody, K. W. Wong, G. Wang, and W. Ela, "A review of irregular time series data handling with gated recurrent neural networks," *Neurocomputing*, vol. 441, pp. 161–178, Jun. 2021.
[16] Y. Liang, Z. Chen, G. Liu, and M. Elgendi, "A new, short-recorded photoplethysmogram dataset for blood pressure monitoring in China," *Sci. Data*, vol. 5, no. 1, pp. 1–7, Feb. 2018.
[17] *IEEE Standard for Wearable Cuffless Blood Pressure Measuring Devices*, IEEE Standard 1708-2014, 2014, pp. 1–38.
[18] E. O'Brien, J. Petrie, W. Littler, M. de Swiet, P. L. Padfield, K. O'Malley, M. Jamieson, D. Altman, M. Bland, and N. Atkins, "The British hypertension society protocol for the evaluation of automated and semi-automated blood pressure measuring devices with special reference to ambulatory systems," *J. Hypertension*, vol. 8, no. 7, pp. 607–619, Jul. 1990.
[19] W. B. White, A. S. Berson, C. Robbins, M. J. Jamieson, L. M. Prisant, E. Roccella, and S. G. Sheps, "National standard for measurement of resting and ambulatory blood pressures with automated sphygmomanometers," *Hypertension*, vol. 21, no. 4, pp. 504–509, Apr. 1993.
[20] M. Hayati, F. Shama, S. Roshani, and A. Abdipour, "Linearization design method in class-F power amplifier using artificial neural network," *J. Comput. Electron.*, vol. 13, no. 4, pp. 943–949, Aug. 2014.
[21] G. H. Roshani, E. Nazemi, and F. Shama, "Utilizing features extracted from registered ^{60}Co gamma-ray spectrum in one detector as inputs of artificial neural network for independent flow regime void fraction prediction," *MAPAN*, vol. 34, no. 2, pp. 189–196, Jan. 2019.
[22] G. Sadeghi, S. Nazari, M. Ameri, and F. Shama, "Energy and exergy evaluation of the evacuated tube solar collector using Cu_2O/water nanofluid utilizing ANN methods," *Sustain. Energy Technol. Assessments*, vol. 37, Feb. 2020, Art. no. 100578.
[23] G. Sadeghi, A. L. Pisello, S. Nazari, M. Jowzi, and F. Shama, "Empirical data-driven multi-layer perceptron and radial basis function techniques in predicting the performance of nanofluid-based modified tubular solar collectors," *J. Cleaner Prod.*, vol. 295, May 2021, Art. no. 126409.
[24] M. Liu, L.-M. Po, and H. Fu, "Cuffless blood pressure estimation based on photoplethysmography signal and its second derivative," *Int. J. Comput. Theory Eng.*, vol. 9, no. 3, pp. 202–206, 2017.
[25] H. Samimi and H. R. Dajani, "A PPG-based calibration-free cuffless blood pressure estimation method using cardiovascular dynamics," *Sensors*, vol. 23, no. 8, p. 4145, Apr. 2023.
[26] N. Aguirre, E. Grall-Maes, L. J. Cymberknop, and R. L. Armentano, "Blood pressure morphology assessment from photoplethysmogram and demographic information using deep learning with attention mechanism," *Sensors*, vol. 21, no. 6, p. 2167, Mar. 2021.
[27] S. Shimazaki, H. Kawanaka, H. Ishikawa, K. Inoue, and K. Oguri, "Cuffless blood pressure estimation from only the waveform of photoplethysmography using CNN," in *Proc. 41st Annu. Int. Conf. IEEE Eng. Med. Biol. Soc. (EMBC)*, Jul. 2019, pp. 5042–5045.
[28] Y.-H. Li, L. N. Harfiya, and C.-C. Chang, "Featureless blood pressure estimation based on photoplethysmography signal using CNN and BiLSTM for IoT devices," *Wireless Commun. Mobile Comput.*, vol. 2021, pp. 1–10, Nov. 2021.
[29] S. González, W.-T. Hsieh, and T. P.-C. Chen, "A benchmark for machine-learning based non-invasive blood pressure estimation using photoplethysmogram," *Sci. Data*, vol. 10, no. 1, Mar. 2023, Art. no. 149.

SYAMSUL RIZAL (Member, IEEE) was born in Bandung, West Java, Indonesia, in August 1988. He received the bachelor's degree from Telkom University, Indonesia, in 2011, and the master's and Ph.D. degrees from the Department of IT Convergence, Kumoh National Institute of Technology, South Korea, in 2018.

During the Ph.D. studies, he notably served as the Team Leader with the Networked Systems Laboratory and engaged in various projects encompassing ISA100.11a; virtualization, image, and video processing; and the Internet of Things (IoT). Since August 2019, he has been an Assistant Professor with the Faculty of Electrical Engineering, Telkom University, Indonesia, where he specializes in developing machine learning algorithms for tea leaf classification. Since September 2023, he has also been a Postdoctoral Researcher with the ICT Convergence Research Center, Kumoh National Institute of Technology, South Korea. He is a Distinguished Academic and a Researcher. He has made significant contributions through his publications, including "Soil Water Content Estimation with the Presence of Vegetation Using Ultra-Wideband Radar-Drone," featured in IEEE Access, in 2022. His work in ECG signal analysis, particularly the "Implementation of One-Dimensional Convolutional Neural Network for Individual Identification Based on ECG Signal," is also noteworthy. Notable projects led by him include the development of a system for estimating soil water content in the presence of vegetation using an ultra-wideband radar drone, funded by a grant from LPDP (Indonesian government), and a project focusing on nutrient deficiency prediction in tea leaves through machine learning. His research interests include the development of blockchain technology integrated with artificial intelligence, machine learning, and AI in biomedical applications.

YUNIARTI ANA RAHMA (Member, IEEE) was born in Kendal, Central Java, Indonesia, in July 1990. She received the B.Eng. degree from the School of Electronic and Electrical Engineering, Telkom University, Bandung, Indonesia, in 2014, and the M.Eng. degree from the Department of IT Convergence Engineering, Kumoh National Institute of Technology, Gumi, South Korea, in 2017, where she is currently pursuing the Ph.D. degree. She is also a Lecturer with the Department of Computer Engineering, Universitas Pendidikan Indonesia (UPI), Indonesia. Her research interest includes AI in biomedical applications.